Sequential delivery of LAIV and SARS-CoV-2 in the ferret model can reduce SARS-CoV-2 shedding and does not result in enhanced lung pathology.

Kathryn A. Ryan[1†], Katarzyna E. Schewe[2†]*, Jonathan Crowe[2], Susan A. Fotheringham[1], Yper Hall[1], Richard Humphreys[1], Anthony C. Marriott[1], Jemma Paterson[1], Emma Rayner[1], Francisco J. Salguero[1], Robert J. Watson[1], Catherine J. Whittaker[1], Miles W. Carroll[1,3], Oliver Dibben[2]

[1]UK Health Security Agency, Porton Down, Salisbury, Wiltshire, United Kingdom SP4 0JG

[2]Flu-BPD, BioPharmaceuticals Development, R&D, AstraZeneca, Liverpool, UK

[3]Nuffield Department of Medicine, Oxford University, Oxford, OX1 3SY, UK

*Corresponding author: Katarzyna E. Schewe, Flu- Biopharmaceutical Development, R&D, AstraZeneca, Liverpool, L24 9JW, UK

Tel:+44 151 485 7413; Email: schewek@astrazeneca.com

[†]These authors contributed equally to this work.

Summary

LAIV administration in proximity to SARS-CoV-2 infection was investigated in ferrets. Vaccination did not exacerbate mild COVID-19 disease and, if delivered pre-challenge, reduced SARS-CoV-2 shedding. This supports safe LAIV administration during the COVID-19 pandemic, with potential to reduce SARS-CoV-2 transmission.

Abstract

Co-circulation of SARS-CoV-2 and influenza viruses could pose unpredictable risks to health systems globally, with recent studies suggesting more severe disease outcomes in co-infected patients. The initial lack of a readily available COVID-19 vaccine has reinforced the importance of influenza vaccine programmes during the COVID-19 pandemic. Live Attenuated Influenza Vaccine (LAIV) is an important tool in protecting against influenza, particularly in children. However, it is unknown whether LAIV administration influences the outcomes of acute SARS-CoV-2 infection or disease. To investigate this, quadrivalent LAIV was administered to ferrets 3 days pre- or post-SARS-CoV-2 infection. LAIV administration did not exacerbate SARS-CoV-2 disease course or lung pathology with either regimen. Additionally, LAIV administered prior to SARS-CoV-2 infection significantly reduced SARS-CoV-2 replication and shedding in the upper respiratory tract. This study demonstrated that LAIV administration in close proximity to SARS-CoV-2 infection does not exacerbate mild disease and can reduce SARS-CoV-2 shedding.

Keywords: live attenuated influenza vaccine, LAIV, SARS-CoV-2, COVID-19, co-infection, ferret

Introduction

The prospect of severe acute respiratory syndrome coronavirus 2 (SARS-CoV-2) co-circulation with other respiratory viruses, particularly influenza virus, has raised major concerns over increased stresses to healthcare systems. Data from UK patients during the first COVID-19 wave showed that SARS-CoV-2 and influenza co-infection correlated with greater risk of severe illness and death [1]. Similar observations were made in rodent models, where sequential influenza and SARS-CoV-2 infection resulted in exacerbated disease pathology [2, 3].

Influenza vaccination remains of paramount importance in mitigating the risks associated with co-circulation of these viruses, particularly for populations not covered by COVID-19 vaccination programmes.

FluMist/Fluenz live attenuated influenza vaccine (LAIV) is primarily used in children, offering individual protection and reduced community influenza transmission [4-9]. LAIV can be administered to children with mild fever, cold, or cough, as there is no evidence of LAIV exacerbating pre-existing mild infections [10-15]. However, the current COVID-19 pandemic raises the possibility of LAIV administration to SARS-CoV-2 infected children displaying either mild or no COVID-19 symptoms [16-18]. Alternatively, SARS-CoV-2 infection could be acquired following LAIV delivery. Due to the replication-competent nature of LAIV and its intranasal delivery, co-incident LAIV and SARS-CoV-2 replication is feasible. Currently there are no clinical data demonstrating this putative interaction or any impact on the resulting COVID-19 illness in children.

An optimized ferret efficacy model for LAIV was recently described [19]. This study identified the importance of a low, ferret-appropriate vaccine dose in the investigation of LAIV in recapitulating clinical vaccine effectiveness. Ferrets have also been shown to provide a model of COVID-19 disease, with mild clinical signs, consistent lung pathology and upper respiratory tract (URT) shedding of SARS-CoV-2 [20-22]a surrogate for the mild to moderate disease seen in clinical cases of COVID-19

[23]. Here, combining these approaches we examined the impact of LAIV administration on pre-existing SARS-CoV-2 infection and associated respiratory pathology in ferrets. We also evaluated the effect of LAIV given prior to SARS-CoV-2 infection.

In sequentially infected animals, we aimed to assess the impact of LAIV on SARS-CoV-2-related histopathology, SARS-CoV-2 viral levels in tissues and SARS-CoV-2 URT shedding as representative indicators of mild COVID-19 disease [22]. Overall, we intended to understand whether LAIV might exacerbate or ameliorate SARS-CoV-2 infection and disease when delivered before or after challenge.

Methods

Cells and viruses

SARS-CoV-2 strain Victoria/01/2020 [24] was generously provided by The Doherty Institute, Melbourne, Australia at P1 after primary growth in Vero/hSLAM cells and subsequently passaged twice at UK Health Security Agency (UKHSA), Porton in Vero/hSLAM cells (ECACC 04091501) as described previously [22].

The quadrivalent LAIV (QLAIV) used was representative of the 2017-18 vaccine and was generated from non-commercial material. Vaccine viruses A/H1N1pdm09 – A/Slovenia/2903/2015, H3N2 – A/New Caledonia/71/2014, B/Yamagata – B/Phuket/3073/2013, B/Victoria – B/Brisbane/60/2008 were propagated as previously described [19, 25, 26]. LAIV was titrated by Fluorescent Focus Assay (FFA) as previously described [27]. Madin–Darby canine kidney (MDCK) cells used in FFA were obtained from American Type Culture Collection (ATCC) and maintained in Eagle's minimum essential medium with non-essential amino acids at 37°C and 5% CO_2, as previously described [27].

Ferrets

All animal work was conducted at UKHSA, Porton Down. Thirty-six healthy, female ferrets (*Mustela putorius furo*) aged 7 months were obtained from a UK Home Office accredited supplier (Highgate Farm, UK). All experimental work was conducted under the authority of a UK Home Office approved project license subjected to local ethical review at UKHSA, Porton Down by the Animal Welfare and Ethical Review Body (AWERB) as required by the *Home Office Animals (Scientific Procedures) Act 1986*.

Ferrets were confirmed seronegative for circulating H1N1, H3N2, and B viruses by hemagglutination inhibition (HAI) assay and SARS-CoV-2 by ELISA. Ferrets were randomly assigned to study groups.

Study Design

On Study Day 0 the ferrets were lightly sedated with isoflurane and intranasally challenged with a 1.0 ml (~0.5 ml/naris) dose of SARS-CoV-2. Groups received either mock challenge (phosphate buffered saline, Gibco, cat. 10010023) or SARS-CoV-2 at 6.7 $\log_{10}$ plaque forming units (PFU)/animal in the same sample diluent. LAIV was administered intranasally under sedation with isoflurane at day -3 or 3 with a single 0.2 ml (~0.1 ml/naris) dose. Groups received either mock vaccination (phosphate buffered saline (ThermoFisher Scientific, Waltham, Massachusetts, USA) with 1x sucrose phosphate (ThermoFisher Scientific: custom product, cat. AC10210390) and 1x gelatine-arginine-glutamate (ThermoFisher Scientific: custom product, cat. AC10207676) or LAIV at 4.0 $\log_{10}$ Fluorescent Focus Units (FFU)/strain/animal, in the same sample diluent.

Throat swabs were taken daily on days 1 to 6 post SARS-CoV-2 challenge. Animals were sedated with isoflurane and a flocked swab (Copan, cat. 552C) was gently stroked across the back of the pharynx in the tonsillar area.

Six ferrets from all groups were euthanized at day 6 post SARS-CoV-2 challenge. Ferrets were anaesthetized with an intramuscular injection of ketamine/xylazine (17.9 mg/kg and 3.6 mg/kg bodyweight) and exsanguination was effected via cardiac puncture, followed by injection of an anesthetic overdose (sodium pentabarbitone Dolethal, Vetquinol UK Ltd, 140 mg/kg). Lower left lung lobe and nasal turbinate were collected into RNAprotect (Qiagen, cat. 76163). Remaining lung tissue and nasal cavity tissue (NCT) were placed in 10% neutral buffered formalin for histopathological analysis. The remaining 4 ferrets from all groups, with the exception of SARS-CoV-2 only, were bled at day 14 and 21 post LAIV administration.

Due to ethical considerations laid out under the NC3Rs framework in the United Kingdom, in particular focusing on minimising the number of animals used in studies, the SARS-CoV-2 only group consisted of 6 ferrets as it was not tested for LAIV induced seroconversion. Additionally, no group of naive ferrets was included for pathology comparison in the study. The ferret model has been utilized widely in infectious disease research and the nature and frequency of typical, incidental background lesions observed in these tissues are well appreciated [28-32].

Pathological Studies

Lung lobes and NCT were fixed by immersion in 10% neutral-buffered formalin, processed and embedded into paraffin wax. NCT samples were decalcified using an EDTA-based solution prior to embedding. Sections of 4 µm were cut and stained with hematoxylin and eosin (HE) and examined microscopically. A NCT and lung histopathology scoring system was used to evaluate histopathological lesions (Supplementary Table 1). Sections were analyzed blinded by 2 qualified veterinary pathologists. In addition, samples were stained using RNAscope to identify SARS-CoV-2 viral RNA. Briefly, tissues were pre-treated with hydrogen peroxide for 10 minutes at room temperature (RT), target retrieval for 15 minutes (98-101°C) and Protease Plus for 30 minutes (40°C) (Advanced Cell Diagnostics). A V-nCoV2019-S probe (Advanced Cell Diagnostics, cat. 848561) was

incubated on the tissues for 2 hours at 40°C. Amplification of signal was carried out following the RNAscope protocol using the RNAscope 2.5 HD Detection kit – Red (Advanced Cell Diagnostics). Digital image analysis was performed on RNAscope labelled slides to ascertain the percentage of stained cells within the lesions, using the Nikon-NIS-Ar package. One section per lung lobe and 2 NCT sections were assessed. NCT sections covered the whole structure.

RT-qPCR

RNA extraction

Throat swab samples were inactivated in AVL (Qiagen) and ethanol. Tissues were homogenized in Buffer RLT+ beta-mercaptoethanol (Qiagen). Homogenate was then centrifuged through a QIAshredder homogenizer (Qiagen) and supplemented with ethanol. Extraction was then performed using the BioSprint™96 One-For-All vet kit (Indical) and Kingfisher Flex platform as per manufacturer's instructions.

SARS-CoV-2 Viral RNA Quantification

Reverse transcription-quantitative polymerase chain reaction (RT-qPCR) targeting a region of the SARS-CoV-2 nucleocapsid (N) gene was used to determine viral loads and was performed using TaqPath™ 1-Step RT-qPCR Master Mix, CG (Applied Biosystems™), 2019-nCoV CDC RUO Kit (Integrated DNA Technologies) and QuantStudio™ 7 Flex Real-Time PCR System. RT-qPCR primers and probe, cycling conditions and detection limits are summarized in Supplementary Table 2.

Hemagglutination Inhibition Assay (HAI)

Ferret antiserum (200 µl) was added to 600 µl receptor-destroying enzyme (Deben Diagnostics, Ipswich, UK) and incubated at 37°C for 18–20 hours. The sera were then heat-inactivated at 56°C for 45 minutes. Treated sera were serially diluted 1:2 and added to an equal volume of virus (8

HAU/well). Virus/antibody complexes were incubated at RT for 30–40 minutes before addition of 1 well-volume of 0.5% chicken (H1N1 and B) or guinea pig (H3N2) red blood cell suspension. The resulting mixture was incubated at RT for 60 minutes and HAI endpoints recorded as the reciprocal of the highest dilution of antiserum able to fully prevent agglutination.

Quantification and statistical analysis

Virus in tissues was measured by RT-qPCR at day 6 post-challenge (pc) and the viral loads were expressed as $\log_{10}$ values. For throat swabs, the geometric mean of RT-qPCR copy numbers for days 1-6 pc was taken for each animal and expressed as a single $\log_{10}$ value to summarize shedding over time. Statistical analysis was performed in JMP v16.1 (SAS Institute Inc.). Statistical significance is shown on figures by horizontal lines and p-value indicators: $^{ns}p>0.05$, *$p<0.05$, **$p<0.01$, further details of tests applied are given in legends.

Results

To assess the implications of LAIV and SARS-CoV-2 co-infection and its impact on COVID-19 disease severity, SARS-CoV-2 was administered intranasally to groups of 6 or 10 ferrets at 6.7 $\log_{10}$ PFU/dose and QLAIV at 4.0 $\log_{10}$ FFU/dose/strain (Figure 1a). LAIV was administered either 3 days before (LAIV/SARS-CoV-2) or 3 days after (SARS-CoV-2/LAIV) the SARS-CoV-2 challenge (Figure 1b). Control groups for SARS-CoV-2 only (Mock/SARS-CoV-2) and LAIV only (LAIV/Mock) were also included. All study groups are summarized in Figure 1c. The endpoints of the study were the histopathological examination of lung and NCT and the quantification of SARS-CoV-2 viral RNA in throat swabs, NCT and lung tissues.

Based on previous observations, a period of 6 days post SARS-CoV-2 infection was chosen to enable assessment of both histopathological changes in respiratory tract and SARS-CoV-2 shedding in URT [22]. As shedding of both QLAIV and SARS-CoV-2 have previously been detected at 3 days post-

infection [19, 22], an interval of 3 days between administration of LAIV and SARS-CoV-2 was applied to ensure that the initial virus inoculum was actively replicating at the time of the subsequent infection.

To demonstrate successful LAIV delivery, 4 ferrets from each LAIV group (SARS-CoV-2/LAIV, LAIV/SARS-CoV-2 and LAIV/Mock) were used to confirm seroconversion post-vaccination. Serum samples were taken at days 14 and 21 post-vaccination, as well as prior to study start (day -5). Seroconversion against the B-Yamagata vaccine strain, B/Phuket/3073/2013, was confirmed by HAI assay in 100% of animals (Supplementary Figure 1).

Histopathological examination showed no effect of LAIV on SARS-CoV-2 lung pathogenesis and only a mild increase in the nasal cavity. Six ferrets from each study group were euthanized 6 days after SARS-CoV-2 challenge and pathological changes were assessed in all lung lobes and NCT.

In NCT, inflammatory and degenerative changes were observed in the mucosa which were similar in appearance for examined animals in all groups (Figure 2, Supplementary Table 3). Animals coinfected with SARS-CoV-2 and LAIV, either LAIV post SARS-CoV-2 challenge (SARS-CoV-2/LAIV) (Figure 2a) or LAIV pre-SAR-CoV-2 challenge (LAIV/SARS-CoV-2) (Figure 2b) had inflammation and degenerative changes. Severity was slightly lower in animals that either received a mock vaccine prior to SARS-CoV-2 challenge (Mock/SARS-CoV-2) (Figure 2c) or LAIV prior to mock challenge (LAIV/Mock) (Figure 2d).

Variable levels of staining for the presence of SARS-CoV-2 RNA were detected in epithelial and sustentacular cells and cellular exudates in 5 of 6 animals that received LAIV post-SARS-CoV-2 challenge (SARS-CoV-2/LAIV) (Figure 2e) and in 4 out of 6 animals that received mock vaccine pre-SARS-CoV-2 challenge (Mock/SARS-CoV-2) (Figure 2g). Staining was absent in all animals that

received LAIV pre-SARS-CoV-2 challenge (LAIV/SARS-CoV-2) (Figure 2f) and in all LAIV only control animals (LAIV/Mock) (Figure 2h).

In the lungs, microscopic inflammatory changes involving both parenchyma and airways were observed in all animals (Supplementary Figure 2); all lobes exhibited a multifocal patchy-to-diffuse distribution of lesions. The overall severity of these lesions was low to mid-grade and similar for all 4 groups (Figure 3a and 3b). No significant differences were observed between lung pathology scores of any of the groups (Figure 3b, Supplementary Table 3). No SARS-CoV-2 RNA was detected in the lungs of any animal.

The NCT pathology score sums for each animal were compared by study group (Figure 3c). No significant difference was observed between Mock/SARS-CoV-2 and LAIV/Mock groups. SARS-CoV-2/LAIV and LAIV/SARS-CoV-2 group scores were both significantly higher than Mock/SARS-CoV-2 group ($p=0.0256$ and $p=0.0006$, respectively). However, their severity was still classified as mild to moderate.

Viral shedding post-challenge in throat swabs was reduced in animals receiving LAIV before SARS-CoV-2. SARS-CoV-2 viral RNA was detected in throat swabs from day 1 pc in the SARS-CoV-2 only group (Mock/SARS-CoV-2). Shedding reached a peak at day 3 pc, with a titre of 5.85 $\log_{10}$ copies/ml and remained consistent until day 6 pc (Supplementary Figure 3). The geometric mean of shedding per day for each group is shown in Figure 4a. In Mock/SARS-CoV-2 animals mean shedding was 4.98 $\log_{10}$ copies/ml/day. The mean shedding in LAIV primed ferrets (LAIV/SARS-CoV-2) was significantly reduced to 4.08 $\log_{10}$ copies/ml/day ($p=0.0153$), while no significant change was noted in SARS-CoV-2/LAIV ferrets (4.43 $\log_{10}$ copies/ml/day ($p=0.37$) (Figure 4a).

SARS-CoV-2 viral RNA levels in lung and NCT homogenates. No SARS-CoV-2 viral RNA was detected in the lungs of any ferret at 6 days post-SARS-CoV-2 challenge. SARS-CoV-2 viral RNA was detected in the NCT of all ferrets challenged with SARS-CoV-2. The SARS-CoV-2/LAIV animals showed no difference in NCT RNA levels relative to the Mock/SARS-CoV-2 group, while the LAIV/SARS-CoV-2 group showed a trend for lower levels of NCT viral RNA when compared to both SARS-CoV-2/LAIV and Mock/SARS-CoV-2 groups. However, this difference was not statistically significant. Ferrets in the LAIV/Mock group were negative for SARS-CoV-2 viral RNA (Figure 4b).

Discussion

To investigate the effect of LAIV on SARS-CoV-2 replication and pathology we applied the ferret model for mild SARS-CoV-2 clinical disease described previously [22]. Our assessment used the most distinct SARS-CoV-2-related endpoints representing COVID-19 disease: respiratory tract histopathology, SARS-CoV-2 RNA shedding in throat swabs and SARS-CoV-2 viral load in respiratory tissues. Other potential indicators of COVID-19 disease such as fever or weight loss were not observed by Ryan et al. [22] and so were not measured here. For all animals in the SARS-CoV-2 only group (Mock/SARS-CoV-2), microscopic lesions were most prominent in the NCT and comprised acute to sub-acute inflammatory and degenerative changes. Histopathological changes were also seen in the lungs, but with a lower frequency and severity. These findings agreed with previous challenge studies, with less severe pathological changes in the lower respiratory tract compared to the URT [22]. This reflected the mild COVID-19 progression typically seen in children [17, 18]. Mild histopathological changes in lungs and NCT were also noted in animals that received LAIV only (LAIV/Mock). LAIV has an excellent safety profile in clinical studies [10, 15], suggesting that this level of pathology resulted from LAIV-induced immune responses. While LAIV shedding was not measured here due to variable detection at the low dose applied, successful vaccination was confirmed by seroconversion against B/Phuket/3073/2013 (Supplementary Figure 1).

Due to ethical considerations, only control groups for pre-SARS-CoV-2 intervention (LAIV/Mock, Mock/SARS-CoV-2) were included. While mock interventions were unlikely to have any significant impact, irrespective of delivery order, this does highlight a limitation of our study design. As vaccination prior to SARS-CoV-2 infection was considered most likely to affect disease course, controlling for this scenario was prioritised.

Microscopic lesions in lungs of co-infected ferrets (LAIV/SARS-CoV-2 and SARS-CoV-2/LAIV) were primarily low-grade and similar in appearance to the control groups, suggesting that LAIV did not alter the LRT disease phenotype irrespective of the infection schedule. Co-infected ferrets showed significantly higher pathology scores in NCT relative to both SARS-CoV-2 only and LAIV only control groups. This likely reflected the combined immune response to SARS-CoV-2 challenge and LAIV administration. However, pathology in the URT remained mild and, coupled with no observable changes in the lungs, was not considered indicative of an enhanced disease phenotype.

SARS-CoV-2 RNA was not detected by RT-qPCR in the lungs of any animal, supporting the mild pathology observed and confirming previous reports [22, 31, 33]. In SARS-CoV-2 control animals (Mock/SARS-CoV-2), SARS-CoV-2 RNA was readily detected by RT-qPCR in throat swabs and NCT, confirming previous observations [22]. SARS-CoV-2 RNA was also detected in throat swabs and NCT of co-infected animals (SARS-CoV-2/LAIV and LAIV/SARS-CoV-2). While RNA levels in the SARS-CoV-2/LAIV group were similar to SARS-CoV-2 only controls (Mock/SARS-CoV-2), SARS-CoV-2 shedding was significantly reduced in animals that received LAIV prior to SARS-CoV-2 challenge (LAIV/SARS-CoV-2). Although no significant differences were seen between SARS-CoV-2 RNA levels in NCT by RT-qPCR, a trend for a similar reduction in RNA levels in LAIV/SARS-CoV-2 animals was also evident. Taken together, these observations aligned with RNAscope observations of NCT, where RNA staining was present in SARS-CoV-2 only (Mock/SARS-CoV-2) and SARS-CoV-2/LAIV groups but not in

LAIV/SARS-CoV-2 or LAIV only (LAIV/Mock) groups. The lack of detection of viral RNA by RNAscope in LAIV/SARS-CoV-2 group relative to RT-qPCR was most likely due to the nature of the applied detection methods and sample type. While RT-qPCR of tissue homogenates represents a global measurement, RNAscope provides a highly localized view, potentially resulting in lower overall sensitivity. In addition, RT-qPCR and RNAscope targeted different genes, N and S, respectively. N gene was previously shown to be the most abundant transcript among SARS-CoV-2 genes [34], which could have influenced detection levels here.

These data suggested that the administration of LAIV did not enhance SARS-CoV-2 replication in ferrets. Moreover, administration of LAIV 3 days prior to SARS-CoV-2 challenge resulted in a reduction in SARS-CoV-2 shedding in the ferret URT. A similar reduction in SARS-CoV-2 shedding in the clinic could have important implications for transmission across the population [35].

Our findings of reduced SARS-CoV-2 shedding in animals receiving LAIV prior to SARS-CoV-2 align with recent observations in the mouse model, where SARS-CoV-2 viral load in the lungs was significantly reduced following an initial wild-type influenza virus infection, when compared to SARS-CoV-2 only infected animals [2]. However, influenza/SARS-CoV-2 co-infected mice displayed more severe disease despite reduced SARS-CoV-2 viral load [2]. This is contrary to our observations for LAIV, showing no evidence of enhanced lung pathology in LAIV/SARS-CoV-2 co-infected ferrets. This distinction was likely due to the higher pathogenicity of wild-type influenza virus relative to LAIV, paired with a more severe COVID-19 disease model in mice. Also, LAIV, unlike wild-type influenza, does not replicate in ferret lungs, as required by safety testing of commercial vaccine, which further distinguishes our observations from the mouse model [36].

We hypothesize that viral competition might play a role in the interaction of LAIV and SARS-CoV-2, as well as LAIV-mediated non-specific immune responses. Previously, LAIV was shown to provide non-specific immediate protection against Respiratory Syncytial Virus infection in mice [37]. In another mouse model LAIV achieved immediate, broad-spectrum protection against heterologous

influenza strains, mediated by antiviral interferon (IFN) responses and pro-inflammatory cytokines [38]. In clinical observations LAIV was protective against an influenza strain that was antigenically distinct from the vaccine strain, within two weeks of vaccination [39]. Zhu et al. investigated transcriptomic changes in whole blood of LAIV vaccinated children and identified clusters of co-expressed genes either modulated by IFN or involved in IFN-regulated pathways. These findings support the establishment of LAIV-induced, IFN-mediated non-specific antiviral immunity in the first few weeks post-vaccination [40]. Use of an unrelated live vaccine, such as measles, mumps, and rubella (MMR), as a preventive measure against COVID-19 has been proposed for similar reasons [41, 42]. However, the amplitude and duration of LAIV-mediated non-specific protection is unclear and clinical data on COVID-19 disease in the context of LAIV uptake could further this understanding.

Whether driven by viral competition or activation of non-specific immune responses, LAIV-mediated reduction in SARS-CoV-2 viral load and shedding is likely to be dependent on the proximity of the two infections. Here, a 3-day interval was used to ensure active replication of the first viral inoculum by the time the second was administered. This inhibitory effect could decline with longer intervals and further work is required to understand its duration. Relative doses of the two competing infections may also be relevant. While an optimized low LAIV dose was used here, concurrent use of a lower SARS-CoV-2 challenge dose, more in keeping with a putative natural exposure, might result in more distinct inhibition by LAIV.

It is worth noting that the SARS-CoV-2 Victoria/01/2020 strain used differs from the currently dominant SARS-CoV-2 delta variant. Similarly, three of the strains in the 2017-18 QLAIV applied here differ from 2021/2022 formulation. While our findings are unlikely to be strain-specific, this would benefit from further exploration.

In addition, the potential impact of SARS-CoV-2 infection on LAIV effectiveness was outside the scope of the present work but must also be considered. Investigations into this important question are ongoing.

Our findings deliver the first evidence that LAIV does not exacerbate the mild pathogenic changes caused by SARS-CoV-2 in the LRT of ferrets when delivered shortly pre- or post-challenge. Moreover, if administered 3 days pre-SARS-CoV-2 infection, LAIV reduced SARS-CoV-2 viral shedding in the URT, raising the possibility of reduced transmission, although this would require dedicated transmission studies to establish.

This work supports the administration of LAIV to children of unknown COVID-19 status and suggests a potential additional benefit of LAIV administration during the COVID-19 pandemic.

Funding Disclosure

This work was supported by AstraZeneca.

Acknowledgments

We thank Sarah Woods for FFA titration of vaccine formulations. We thank Laura Hunter and Chelsea Kennard for providing Histology support and expertise. Thank you to Marilyn Aram, Alastair Handley, Daniel Knott, Breeze Cavell, Stephen Thomas, Oliver Skinner and Thomas Bean for assistance with sample processing and all Biological Investigations Group staff for animal husbandry and assistance with in vivo procedures.

Conflicts of interests

At the time of data generation for this publication, Katarzyna E. Schewe, Jonathan Crowe and Oliver Dibben were employees and shareholders of AstraZeneca plc. AstraZeneca plc are the manufacturers of Fluenz® Tetra/FluMist® Quadrivalent intranasal influenza live virus vaccine.

Contributions

Conceptualization: O.D., A.C.M., M.W.C., C.J.W.

Methodology: K.A.R., K.E.S.

Investigation: K.A.R., J.P., R.W., J.F.S., E.R., S.F., R.H.

Formal Analysis: K.A.R., K.E.S., J.C., J.P., R.W., J.F.S., E.R.

Writing Original Draft: K.A.R., K.E.S.

Visualization: K.A.R., K.E.S.

Supervision: K.A.R., K.E.S., O.D.

Project Administration: O.D., K.E.S., K.A.R., Y.H., C.J.W.

Funding Acquisition: O.D.

Review & Editing: all authors

Figures and tables

Figure 1. Study design for assessment of impact of LAIV on SARS-CoV-2 infection in ferrets. (a) Viral strains for quadrivalent LAIV formulation with 4.0 log_{10} FFU/dose/strain and SARS-CoV-2 with 6.7 log_{10} PFU/dose. **(b)** LAIV and SARS-CoV-2 were sequentially administered to groups of 10 or 6 ferrets intranasally. SARS-CoV-2 infection occurred at day 0 (d0) and LAIV was administered at day 3 or -3. Vertical grey lines indicate throat swabs at days 1, 2, 3, 4, 5 and 6. For histopathological assessment 6 ferrets from each group were culled at day 6. Bleeds for LAIV induced immune responses were taken from the remaining 4 ferrets in all LAIV treated groups (SARS-CoV-2/LAIV, LAIV/SARS-CoV-2 and LAIV/Mock) 14 or 21 days post LAIV. **(c)** Four groups of 10 (SARS-CoV-2/LAIV, LAIV/SARS-CoV-2 and LAIV/Mock) or 6 (Mock/SARS-CoV-2) ferrets were included. LAIV was administered either post SARS-CoV-2 challenge (SARS-CoV-2/LAIV) or pre SARS-CoV-2 challenge (LAIV/SARS-CoV-2). Control groups received either mock LAIV and SARS-CoV-2 (Mock/SARS-CoV-2) or LAIV and mock SARS-CoV-2 (LAIV/Mock).

Figure 2. Histopathological changes and SARS-CoV-2 RNA detection in the nasal cavity. a) Group SARS-CoV-2/LAIV; **b)** Group LAIV/SARS-CoV-2; **c)** Group Mock/SARS-CoV-2 and **d)** Group LAIV/Mock. Microscopic inflammatory changes with variable epithelial degeneration and loss and exudate. 200 x magnification, insets 800 x magnification. (HE). Viral staining for SARS-CoV-2 RNA is positive in **e)** Group SARS-CoV-2/LAIV; and **g)** Group Mock/SARS-CoV-2, and absent in **f)** Group LAIV/SARS-CoV-2; and **h)** Group LAIV/Mock. 200 x magnification.

Figure 3. Histopathological examination of lung and nasal cavity tissue shows no impact of LAIV on SARS-CoV-2 lung pathology. Lung and nasal cavity tissue samples were taken from all ferrets at day 6 post-challenge and inflammation-related parameters were examined: epithelial inflammation and degeneration in nasal cavity tissue and inflammation (Infl.) of alveolar walls/spaces, perivascular (PV) lymphocytic cuffing, bronchiolar inflammation and bronchial inflammation in lung tissue. **(a)** Changes were scored from 0 (normal), 1 (minimal), 2 (mild), 3 (moderate) to 4 (marked) for each ferret and summarized in the heat map. **(b)** Lung scores were compared. Symbols indicate the sum of pathology scores per ferret and bars show the group means with standard deviation. **(c)** Nasal cavity tissue scores were compared. Symbols indicate epithelial inflammation and degeneration in nasal cavity tissue and bars show the group means with standard deviation. One-way ANOVA was followed by Dunnett's test with Mock/SARS-CoV-2 used as a control comparator. Statistical significance is shown by horizontal lines and p-value indicators: $^{ns}p > 0.05$, $*p < 0.05$, $**p < 0.01$.

Figure 4. SARS-CoV-2 viral RNA detection in throat swabs and nasal cavity tissue. (a) The throat swabs were taken at days 1, 2, 3, 4, 5 and 6 post-challenge and SARS-CoV-2 viral loads were determined by RT-qPCR. The symbols show the geometric mean of virus titres over 6 days for 1 ferret, bars represent the group mean of 10 (SARS-CoV-2/LAIV, LAIV/SARS-CoV-2 and LAIV/Mock) or 6 (Mock/SARS-CoV-2) ferrets with standard deviation. Due to absence of SARS-CoV-2 infection, LAIV/Mock was treated as a qualitative control only and excluded from statistical analysis. A Kruskal-Wallis test was followed by Dunn's test with Mock/SARS-CoV-2 used as a control comparator. Statistical significance is shown by horizontal lines and P-value indicators: $^{ns}p > 0.05$, $*p < 0.05$. Horizontal dotted lines show the lower limit of quantification (LoQ=4.11 $\log_{10}$ RNA copies/ml/day) and the lower limit of detection (LoD=3.47 $\log_{10}$ RNA copies/ml/day). Excluding LAIV/Mock, the lower 95% confidence limit of all group means was >LoD. **(b)** SARS-CoV-2 RNA was measured in nasal

cavity tissue homogenates by RT-qPCR. The symbols show the viral load measured in nasal cavity tissue at day 6 for each ferret, bars represent the group mean of 6 ferrets with standard deviation. LAIV/Mock was treated as a qualitative control only and excluded from statistical analysis, which was by one-way ANOVA only. Comparison lines showing $^{ns}p > 0.05$ are shown for reference only (no post-test was done). Horizontal dotted lines show the lower limit of quantification (LoQ=4.76 $\log_{10}$ RNA copies/g) and the lower limit of detection (LoD=4.12 $\log_{10}$ RNA copies/g). Excluding LAIV/Mock, the lower 95% confidence limit of all group means was >LoD.

References

1. Stowe J, Tessier E, Zhao H, et al. Interactions between SARS-CoV-2 and influenza, and the impact of coinfection on disease severity: a test-negative design. Int J Epidemiol. **2021**; 50:1124-33.

2. Clark JJ, Penrice-Randal R, Sharma P, et al. Sequential infection with influenza A virus followed by severe acute respiratory syndrome coronavirus 2 (SARS-CoV-2) leads to more severe disease and encephalitis in a mouse model of COVID-19. **2020**:2020.10.13.334532.

3. Zhang AJ, Lee AC, Chan JF, et al. Coinfection by Severe Acute Respiratory Syndrome Coronavirus 2 and Influenza A(H1N1)pdm09 Virus Enhances the Severity of Pneumonia in Golden Syrian Hamsters. Clin Infect Dis. **2021**; 72:e978-e92.

4. Ashkenazi S, Vertruyen A, Arístegui J, et al. Superior relative efficacy of live attenuated influenza vaccine compared with inactivated influenza vaccine in young children with recurrent respiratory tract infections. The Pediatr Infect Dis J. **2006**; 25:870-9.

5. Baum U, Kulathinal S, Auranen K, Nohynek H. Effectiveness of 2 Influenza Vaccines in Nationwide Cohorts of Finnish 2-Year-Old Children in the Seasons 2015-2016 Through 2017-2018. Clin Infect Dis. **2020**; 71:e255-e61.

6. Belshe RB, Edwards KM, Vesikari T, et al. Live attenuated versus inactivated influenza vaccine in infants and young children. N Engl J Med. **2007**; 356:685-96.

7. Buchan SA, Booth S, Scott AN, et al. Effectiveness of Live Attenuated vs Inactivated Influenza Vaccines in Children During the 2012-2013 Through 2015-

2016 Influenza Seasons in Alberta, Canada: A Canadian Immunization Research Network (CIRN) Study. JAMA Pediatr. **2018**; 172:e181514.

8. King JC, Jr., Cummings GE, Stoddard J, et al. A pilot study of the effectiveness of a school-based influenza vaccination program. Pediatrics. **2005**; 116:e868-73.

9. Pebody RG, Whitaker H, Ellis J, et al. End of season influenza vaccine effectiveness in primary care in adults and children in the United Kingdom in 2018/19. Vaccine. **2020**; 38:489-97.

10. Caspard H, Steffey A, Mallory RM, Ambrose CS. Evaluation of the safety of live attenuated influenza vaccine (LAIV) in children and adolescents with asthma and high-risk conditions: a population-based prospective cohort study conducted in England with the Clinical Practice Research Datalink. BMJ Open. **2018**; 8:e023118.

11. CDC. Live Attenuated Influenza Vaccine [LAIV] (The Nasal Spray Flu Vaccine). Available at: https://www.cdc.gov/flu/prevent/nasalspray.htm.

12. Duffy J, Lewis M, Harrington T, et al. Live attenuated influenza vaccine use and safety in children and adults with asthma. Ann Allergy Asthma Immunol. **2017**; 118:439-44.

13. Fleming DM, Crovari P, Wahn U, et al. Comparison of the efficacy and safety of live attenuated cold-adapted influenza vaccine, trivalent, with trivalent inactivated influenza virus vaccine in children and adolescents with asthma. The Pediatr Infec Dis J. **2006**; 25:860-9.

14. Ray GT, Lewis N, Goddard K, et al. Asthma exacerbations among asthmatic children receiving live attenuated versus inactivated influenza vaccines. Vaccine. **2017**; 35:2668-75.

15. Turner PJ, Fleming L, Saglani S, Southern J, Andrews NJ, Miller E. Safety of live attenuated influenza vaccine (LAIV) in children with moderate to severe asthma. J Allergy Clin Immunol. **2020**; 145:1157-64.e6.

16. Lanari M, Chiereghin A, Biserni GB, Rocca A, Re MC, Lazzarotto T. Children and SARS-CoV-2 infection: innocent bystanders…until proven otherwise. Clin Microbiol Infect. **2020**; 26:1130-2.

17. Sola AM, David AP, Rosbe KW, Baba A, Ramirez-Avila L, Chan DK. Prevalence of SARS-CoV-2 Infection in Children Without Symptoms of Coronavirus Disease 2019. JAMA Pediatr. **2021**; 175:198-201.

18. Yonker LM, Neilan AM, Bartsch Y, et al. Pediatric Severe Acute Respiratory Syndrome Coronavirus 2 (SARS-CoV-2): Clinical Presentation, Infectivity, and Immune Responses. J Pediatr. **2020**; 227:45-52.e5.

19. Dibben O, Crowe J, Cooper S, Hill L, Schewe KE, Bright H. Defining the root cause of reduced H1N1 live attenuated influenza vaccine effectiveness: low viral fitness leads to inter-strain competition. NPJ Vaccines. **2021**; 6:35.

20. Kim YI, Kim SG, Kim SM, et al. Infection and Rapid Transmission of SARS-CoV-2 in Ferrets. Cell Host Microbe. **2020**; 27:704-9.e2.

21. Shi J, Wen Z, Zhong G, et al. Susceptibility of ferrets, cats, dogs, and other domesticated animals to SARS-coronavirus 2. Science. **2020**; 368:1016-20.

22. Ryan KA, Bewley KR, Fotheringham SA, et al. Dose-dependent response to infection with SARS-CoV-2 in the ferret model and evidence of protective immunity. Nat Commun. **2021**; 12:81.

23. Wölfel R, Corman VM, Guggemos W, et al. Virological assessment of hospitalized patients with COVID-2019. Nature. **2020**; 581:465-9.

24. Caly L, Druce J, Roberts J, et al. Isolation and rapid sharing of the 2019 novel coronavirus (SARS-CoV-2) from the first patient diagnosed with COVID-19 in Australia. Med Jo Aust. **2020**; 212:459-62.

25. Hoffmann E, Mahmood K, Chen Z, et al. Multiple gene segments control the temperature sensitivity and attenuation phenotypes of ca B/Ann Arbor/1/66. J Virol. **2005**; 79:11014-21.

26. Jin H, Lu B, Zhou H, et al. Multiple amino acid residues confer temperature sensitivity to human influenza virus vaccine strains (flumist) derived from cold-adapted a/ann arbor/6/60. Virology. **2003**; 306:18-24.

27. Hawksworth A, Lockhart R, Crowe J, et al. Replication of live attenuated influenza vaccine viruses in human nasal epithelial cells is associated with H1N1 vaccine effectiveness. Vaccine. **2020**; 38:4209-18.

28. Bewley KR, Gooch K, Thomas KM, et al. Immunological and pathological outcomes of SARS-CoV-2 challenge following formalin-inactivated vaccine in ferrets and rhesus macaques. Sci Adv. **2021**; 7:eabg7996.

29. Conforti A, Marra E, Palombo F, et al. COVID-eVax, an electroporated DNA vaccine candidate encoding the SARS-CoV-2 RBD, elicits protective responses in animal models. Mol Ther. **2021**.

30. Lambe T, Spencer AJ, Thomas KM, et al. ChAdOx1 nCoV-19 protection against SARS-CoV-2 in rhesus macaque and ferret challenge models. Commun Biol. **2021**; 4:915.

31. Proud PC, Tsitoura D, Watson RJ, et al. Prophylactic intranasal administration of a TLR2/6 agonist reduces upper respiratory tract viral shedding in a SARS-CoV-2 challenge ferret model. EBioMedicine. **2021**; 63:103153.

32. Ryan KA, Bewley KR, Fotheringham SA, et al. Dose-dependent response to infection with SARS-CoV-2 in the ferret model and evidence of protective immunity. Nat Commun. **2021**; 12:81.

33. Lambe T, Spencer AJ, Thomas KM, et al. ChAdOx1 nCoV-19 protection against SARS-CoV-2 in rhesus macaque and ferret challenge models. Commun Biol. **2021**; 4:915.

34. Finkel Y, Mizrahi O, Nachshon A, et al. The coding capacity of SARS-CoV-2. Nature. **2021**; 589:125-30.

35. Kawasuji H, Takegoshi Y, Kaneda M, et al. Transmissibility of COVID-19 depends on the viral load around onset in adult and symptomatic patients. PloS One. **2020**; 15:e0243597.

36. Maassab HF, Kendal AP, Abrams GD, Monto AS. Evaluation of a cold-recombinant influenza virus vaccine in ferrets. Journal Infect Dis. **1982**; 146:780-90.

37. Lee YJ, Lee JY, Jang YH, Seo SU, Chang J, Seong BL. Non-specific Effect of Vaccines: Immediate Protection against Respiratory Syncytial Virus Infection by a Live Attenuated Influenza Vaccine. Front Microbiol. **2018**; 9:83.

38. Seo SU, Lee KH, Byun YH, Kweon MN, Seong BL. Immediate and broad-spectrum protection against heterologous and heterotypic lethal challenge in mice by live influenza vaccine. Vaccine. **2007**; 25:8067-76.

39. Piedra PA, Gaglani MJ, Kozinetz CA, et al. Trivalent live attenuated intranasal influenza vaccine administered during the 2003-2004 influenza type A (H3N2) outbreak provided immediate, direct, and indirect protection in children. Pediatrics. **2007**; 120:e553-64.

40. Zhu W, Higgs BW, Morehouse C, et al. A whole genome transcriptional analysis of the early immune response induced by live attenuated and inactivated influenza vaccines in young children. Vaccine. **2010**; 28:2865-76.

41. Chumakov K, Benn CS, Aaby P, Kottilil S, Gallo R. Can existing live vaccines prevent COVID-19? Science. **2020**; 368:1187-8.

42. Fidel PL, Jr., Noverr MC. Could an Unrelated Live Attenuated Vaccine Serve as a Preventive Measure To Dampen Septic Inflammation Associated with COVID-19 Infection? mBio. **2020**; 11.

Figure 1

a

LAIV 4.0 $\log_{10}$ FFU/dose/strain	SARS-CoV-2 6.7 $\log_{10}$ PFU/dose
A/Slovenia/2903/2015 A/New Caledonia/71/2014 B/Brisbane/60/2008 B/Phuket/3073/2013	Victoria/1/2020

b

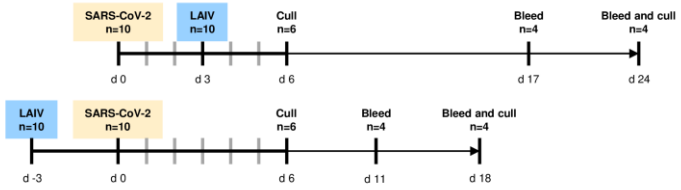

c

Group	LAIV 4.0 $\log_{10}$ FFU/dose/strain	SARS-CoV2 6.7 $\log_{10}$ PFU/dose	LAIV 4.0 $\log_{10}$ FFU/dose/strain
SARS-CoV-2/LAIV (n=10)	-	+	+
LAIV/SARS-CoV-2 (n=10)	+	+	-
Mock/SARS-CoV-2 (n=6)	mock	+	-
SARS-CoV-2/Mock (n=4)	-	+	mock
LAIV/Mock (n=10)	+	mock	-

Figure 2

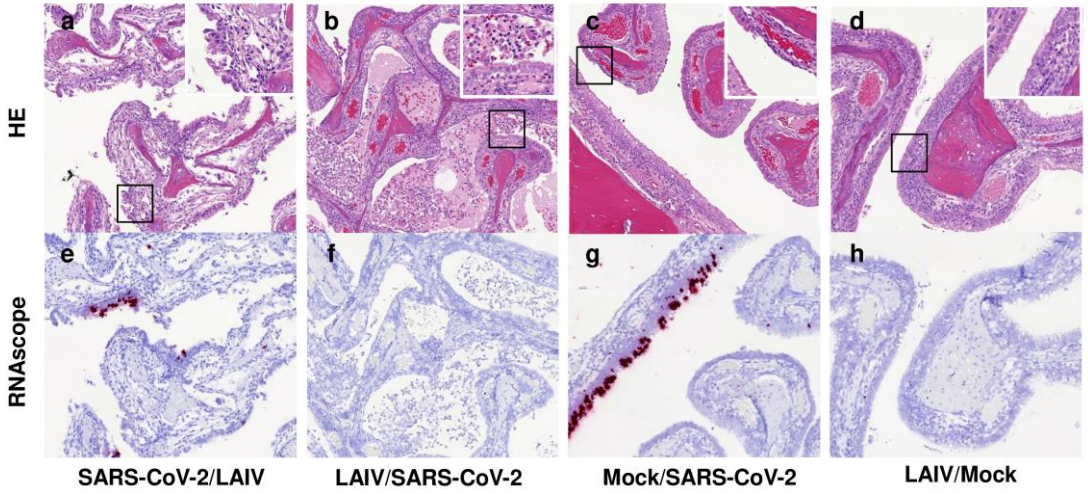
HE
RNAscope
a
b
c
d
e
f
g
h
SARS-CoV-2/LAIV
LAIV/SARS-CoV-2
Mock/SARS-CoV-2
LAIV/Mock

Figure 3

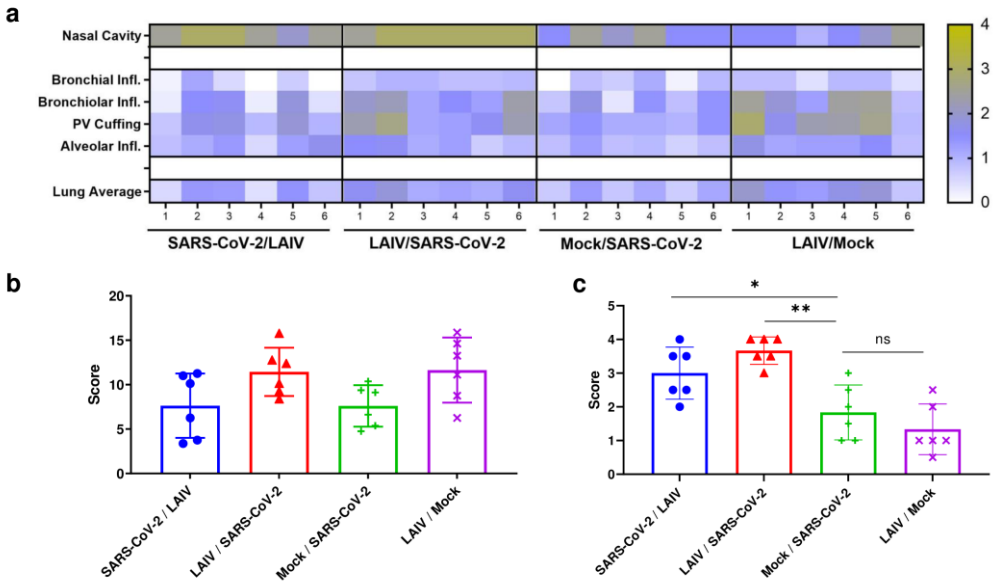
a
Nasal Cavity
Bronchial Infl.
Bronchiolar Infl.
PV Cuffing
Alveolar Infl.
Lung Average
1 2 3 4 5 6
SARS-CoV-2/LAIV
LAIV/SARS-CoV-2
Mock/SARS-CoV-2
LAIV/Mock
4
3
2
1
0
b
Score
20
15
10
5
0
SARS-CoV-2 / LAIV
LAIV / SARS-CoV-2
Mock / SARS-CoV-2
LAIV / Mock
c
*
**
ns
Score
5
4
3
2
1
0
SARS-CoV-2 / LAIV
LAIV / SARS-CoV-2
Mock / SARS-CoV-2
LAIV / Mock

Figure 4

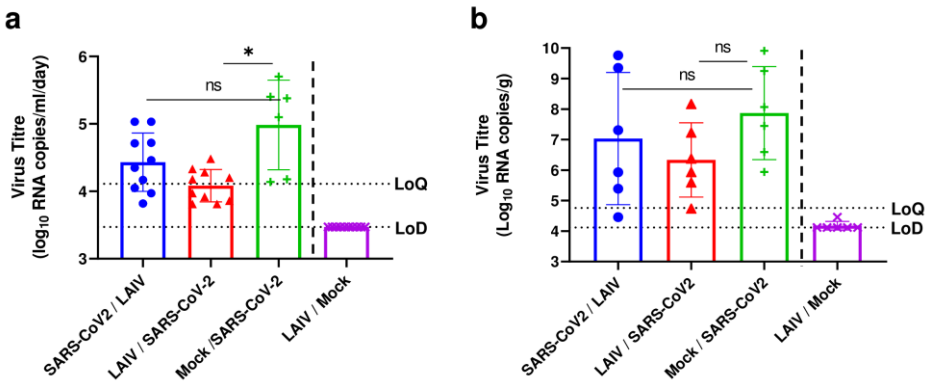
a
Virus Titre
(log10 RNA copies/ml/day)
6
5
4
3
*
ns
LoQ
LoD
SARS-CoV2 / LAIV
LAIV / SARS-CoV-2
Mock /SARS-CoV-2
LAIV / Mock
b
Virus Titre
(Log10 RNA copies/g)
10
9
8
7
6
5
4
3
ns
ns
LoQ
LoD
SARS-CoV2 / LAIV
LAIV / SARS-CoV2
Mock / SARS-CoV2
LAIV / Mock